JOURNAL OF MATERIALS SCIENCE **40** (2005) 3881 – 3886

Review
Thermal—magnetic investigation of the decomposition of copper oxalate—a precursor for catalysts

B. DONKOVA*
Department of Inorganic Chemistry, Faculty of Chemistry, University of Sofia, 1 J.Bourchier Av., Sofia 1164, Bulgaria
E-mail: nhbd@inorg.chem.uni-sofia.bg

D. MEHANDJIEV
Institute of General and Inorganic Chemistry, Bulgarian Academy of Sciences, Acad. G.Bonchev Str. Bl.11, Sofia 1113, Bulgaria
E-mail: metkomeh@svr.igic.bas.bg

A catalyst precursor with highly developed specific surface area of 10 m^2/g and a pore volume of 0.02 cm^3/g is synthesized. The peculiarities of the system studied related to the structure of the copper oxalate, crystallizing as an anhydrous salt with "zeolitic type" bonded water, its content varying between 0 and 1, are pointed out. The thermal decomposition is followed by investigating the magnetic properties in situ. The results are complementary to the information obtained by DTA/TG studies. The performance of magnetic measurements and the calculation of the magnetic moment μ_{eff} in the range from –100 to 300°C allow a conclusion to be drawn concerning the coordination of the Cu(II) ions and the change in the oxidation state. In the starting oxalate, Cu(II) is in a tetrahedral-like coordination, which is a result of the strong tetragonal deformation of the octahedral field and of the stronger tendency of the oxalate ion to rotate around the C–C bond axis. The dehydration process does not affect the XRD results, but changes the temperature dependence of μ_{eff} due to the change in the Cu(II) coordination. The μ_{eff} values during the decomposition process suggest that the proportion Cu(II)-Cu(I) could be varied in the final product by varying the temperature range. By isothermal annealing at 300°C for 1 h, an oxide product containing Cu(II)-Cu(I) is synthesized and characterized. The solid phase products corresponding to the separate parts of the DTA/TG curves are: [Cu] → Cu + Cu_2O (185–300°C), 0.5Cu_2O + 2CuO (300–345°C), 3CuO (345–400°C).

1. Introduction

The sparingly soluble oxalate systems are widely used as precursors in the synthesis of nanomaterials and high-temperature superconductive ceramic materials, containing CuO [1–5] due to the fact that the precipitation processes provide the possibility of controlling the chemical and physical properties of the final products. It is also known that CuO alone or as a part of mixed oxides, as well as deposited on various substrates, is used as a heterogeneous catalyst. The application of oxalate systems in the preparation of catalysts containing CuO is of special interest [6–11].

Copper(II) oxalate, $CuC_2O_4 \cdot nH_2O$ ($0 < n \leq 1$), differs from the other 3d-oxalates $MC_2O_4 \cdot 2H_2O$ (M = Mn, Fe, Co, Ni, and Zn) in several aspects. While the latter contain a fixed amount of crystallization water (usually 2 mol H_2O), the water content in copper oxalate varies between 0 and 1 [12–22] and the bonding is of "zeolitic" type [20]. The obtaining of $CuC_2O_4 \cdot 0.5H_2O$ is most often reported. Furthermore, copper oxalate crystallizes in an orthorhombic syngony, space group Pnnm ($P2_1/c$) [20], and is not isostructural with respect to the dihydrates of Mn, Fe, Co, Ni, and Zn oxalates. In the case of Cu(II) oxalate, a ribbon-like structure is established [16–19] in which, according to Schmittler [19], the copper ions complete their octahedral coordination by oxygen atoms belonging to adjacent ribbons, while in the case of $MC_2O_4 \cdot 2H_2O$ the octahedral coordination of the 3d-cation is completed with the oxygen

*Author to whom all correspondence should be addressed.

atoms from the water molecules. In copper(II) oxalate, however, a disturbance in the octahedral surrounding of the metal ion due to Jahn-Teller distortion can be expected.

The processes of thermal decomposition of $CuC_2O_4 \cdot nH_2O$ are extensively studied [5, 11, 21–28]. In inert atmosphere or vacuum, copper oxalate decomposes to the metal and carbon dioxide [22, 23, 25, 26]. This is in accordance with the generally accepted classifications of Dollimore [29], Boldyrev [30], and Brown [31], based on thermodynamic factors [32]. However, some authors report a mixture Cu + Cu_2O [21] or Cu + CuO [24].

In air atmosphere, the final product is either CuO [4, 5, 21, 25–28] or $CuO_{0.75}$ [11]. Differences exist, however, in the interpretation of the reaction paths. According to some authors, CuO is the product of the oxidation of copper formed during the decomposition [5, 25–28]. Other authors [4] assume that CuO is a decomposition product, formed together with a gas mixture of carbon oxide and dioxide, but this decomposition scheme is typical only of the oxalates of zinc, iron, chromium, and manganese [29–31]. In [33], the assumption is made that the thermal decomposition of copper carboxylates, respectively of oxalate, takes place as a stepwise reduction of the cation according to the scheme $CuC_2O_4 \longrightarrow Cu_2C_2O_4 \longrightarrow CuO$.

It is clear that the reaction path for the preparation of a defined oxide product is a complex process depending on both the experimental conditions (surrounding environment, heating rate, reactant mass, type of crucible) and the possibility of occurrence of secondary processes. In this respect, the effect of the conditions for the preparation of the precursor on its properties and thermal stability should also be mentioned [26]. These are factors influencing substantially the properties of the oxide product obtained. On the other hand, it is known that by varying the concentration of the starting solutions and the crystallization procedure, a crystalline precipitate with differently developed surface area can be obtained, which defines the dispersity of the oxide product obtained. For this reason, it is quite important to set appropriate conditions for the precursor synthesis and to follow its decomposition by comparing different methods. This will elucidate the mechanism of formation of the final product and will provide a possibility of selection of reproducible conditions for the synthesis of an oxide product with desired properties depending on its application.

The present research aims at the preparation of $CuC_2O_4 \cdot nH_2O$ with a highly developed surface and the elucidation of the route of its thermal decomposition by investigating the magnetic properties in situ, as well as the mechanism of the obtaining of the final phase-CuO. The calculation of the magnetic moment enables to monitor changes in the oxidation state of copper(II) and its coordination in the processes of dehydration and decomposition. To the best of our knowledge, such an investigation of these two processes has not been reported in the literature.

2. Experimental

2.1. Synthesis of $CuC_2O_4 \cdot 0.5H_2O$ and oxide product

The $CuC_2O_4 \cdot 0.5H_2O$ sample was obtained by spontaneous crystallization carried out by the simultaneous addition of the reagents in the reaction vessel. The initial reagents were "high purity" grade $CuSO_4 \cdot 5H_2O$ and $K_2C_2O_4 \cdot H_2O$. The concentration of the initial solutions (0.2 mol/dm^3) as well as the precipitation procedure were established by preliminary experiments and aim at the preparation of a precipitate with a highly developed surface area. The preparation conditions were $T = 25^\circ$C, controlled acidity of the medium (pH = 3.0 $\pm$ 0.1) in order to prevent the cation hydrolysis, and continuous stirring of the reaction system. The obtained light blue precipitate was filtered, washed with bidistilled water, and air-dried.

Two samples from the initial oxalate were annealed for 1 h in air at 200 and 300°C, then tempered in a desiccator and weighed.

2.2. Characterization and investigation

2.2.1. X-ray diffraction analysis

The XRD analysis was carried out with a D 500 Siemens powder diffractometer using Cu $K_{\acute{a}}$ radiation in a 2θ diffraction interval of 10–60 degrees. The stepwise scanning was performed with a $0.02^\circ 2\theta$ step and counting time of 2 s/step. The identification of the phases was realized by means of the database JCPDS—International Centre for Powder Diffraction Data.

2.2.2. Thermal analysis

The thermal investigations were performed on a Paulik-Erdey MOM OD-102 derivatograph. The DTA and TG curves were obtained in a static air atmosphere with sample mass of 0.200 g at a heating rate of 10°C/min in the 25–900°C temperature range, using a standard corundum crucible.

2.2.3. Magnetic measurements

The specific magnetic susceptibility of the copper oxalate, as well as that of the resulting oxide, were studied in the temperature range from –100 to 300°C with a Faraday-type magnetic balance. In the course of the in situ monitoring of the process of decomposition, the magnetic measurement was carried out by a stepwise increase of the temperature. At each step, the temperature was kept constant for 30 min before starting the measurements.

The determination of the mass change during the magnetic measurements is indispensable for the calculation of the effective magnetic moments μ_{eff}. The latter were calculated on the basis of the Curie-Weiss law, using the values of the magnetic susceptibilities.

In the case of *in situ* measurements, the magnetic moments were calculated as

$$\mu_{\text{eff}} = 2.828\,[X_M(T-\theta)]^{1/2}, \qquad (1)$$

where X_M is the molar magnetic susceptibility, μ_{eff} is the effective magnetic moment in Bohr's magneton BM; θ is the Weiss constant in K; T is the absolute temperature in K. While the magnetic moment enables the determination of the oxidation state of the metal, the Weiss constant depends on the environment of the given ion and is used to monitor changes in the character of interaction between the metal ions [34–36].

2.2.4. Determination of the surfaces area

BET determinations were carried out by studying the nitrogen sorption at 77.4 K.

3. Results and discussion

3.1. $CuC_2O_4 \cdot 0.5H_2O$ precursor

Fig. 1a shows the X-ray patterns of the starting copper oxalate. The initial sample coincides with JCPDS No 21-0297—orthorhombic structure.

Fig. 2a shows scanning electron micrographs of the starting oxalate. It is seen that the initial phase consists of hollow ellipsoids. The size distribution curve obtained from the data of an electron microscopic study has a maximum in the region 1.6–1.8 μm. In the determination of the specific surface area, an adsorption isotherm of the H1 type (according to the IUPAC classification [37]) is obtained. The copper oxalate sample has a strongly developed surface of 10 m^2/g, with a pore volume of 0.02 cm^3/g. This fact suggests that the chosen method and conditions for carrying out a spontaneous crystallization result in the formation of a highly dispersed precipitate.

In Fig. 3, curve 1, the temperature dependence of the magnetic susceptibility of the oxalate is shown in the range from −100 to 300°C. It is seen that the oxalate is antiferromagnetic and belongs to the systems manifesting a molecular antiferromagnetism. This is also established by other authors [12–16]. Our curve reveals a maximum in the range from −78°C to −50°C, after which the magnetic susceptibility decreases with the rise of temperature up to 300°C. The maximum in the magnetic susceptibility is in good agreement with literature data, taking into account that its location depends on the sample dispersity. It is known [8] that by increasing dispersity, the temperature of the maximum in the curve of the magnetic susceptibility decreases. This fact is well shown in [15] where two samples of copper oxalate with different particle size are investigated. The low temperature range of the maximum obtained in the present study is another confirmation of the high dispersity of the oxalate.

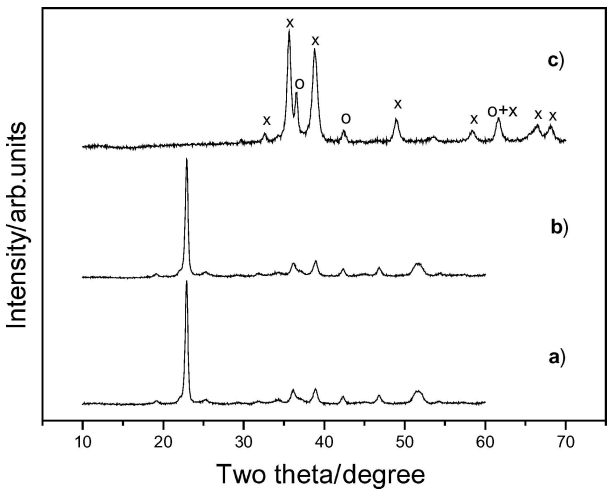

Figure 1 X-ray diffractograms: (a) initial oxalate, JCPDS 21-0297; (b) sample annealed for 1 h at 200°C; (c) sample annealed for 1 h at 300°C (x-CuO, JCPDS 48-1548; o-Cu_2O, JCPDS 78-2076).

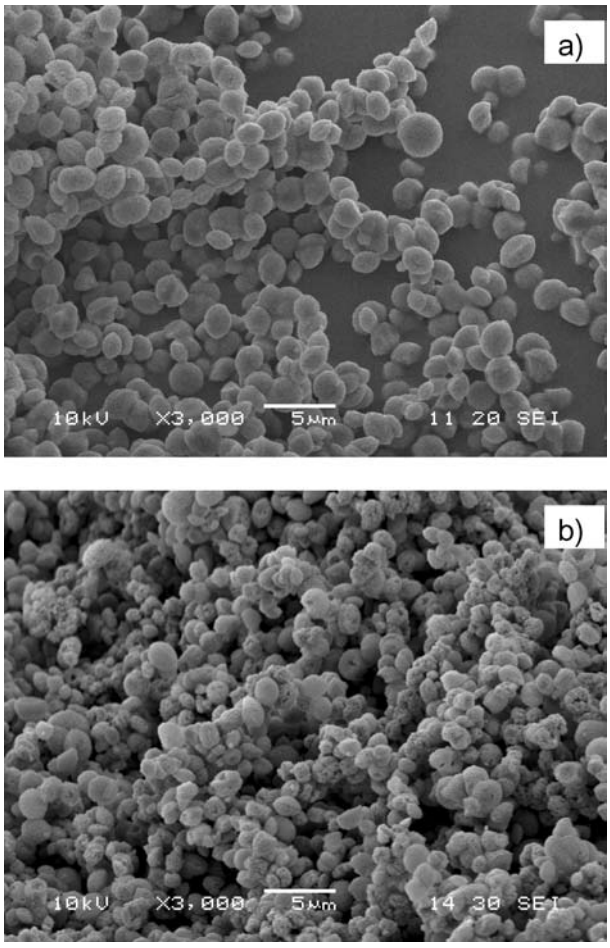

Figure 2 Scanning electron microscope observation of (a) initial copper oxalate; (b) sample, annealed for 1 h at 300°C.

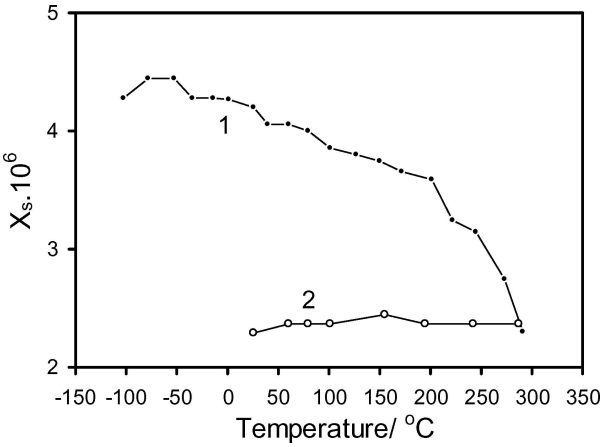

Figure 3 Temperature dependences of the specific magnetic susceptibility of $CuC_2O_4 \cdot 0.5H_2O$ (curve 1) and of the oxide product obtained after annealing for 1 h at 300°C (curve 2).

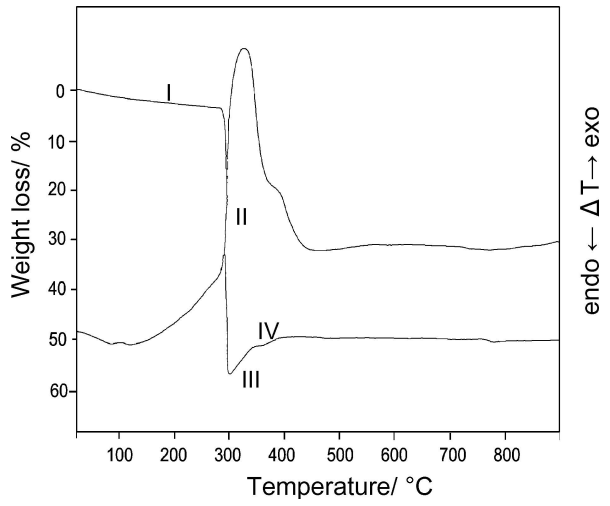

Figure 4 DTA and TG curves of $CuC_2O_4 \cdot 0.5H_2O$.

The results from the DTA and TG analyses are depicted in Fig. 4. Based on the shape of the DTA curve, the copper oxalate decomposition is described in the literature [24, 29] as an autocatalytic process. The TG curve obtained is typical of Cu, Ni, and Co oxalates, according to the classification of the TG curves made by Dollimore [29].

In order to interpret the trend of the curves, one should bear in mind the following peculiarities of the system: 1. Due to the structure and the type of the water bonding, a fully anhydrous copper oxalate cannot be obtained [13–19] and the X-ray pattern is unaffected by the water content [19]. 2. From the thermodynamic point of view, the obtaining of elementary copper is most probable [29–32]. 3. The copper obtained is very "active" and highly reactive, hence it will immediately oxidize. 4. This is a stepwise oxidation through Cu_2O to CuO, the complete transformation occurring beyond 400°C, as it has been established by annealing of a copper foil in air at 5 K/min [26].

The DTA curve shows a very week and broad endothermic effect of partial dehydration, starting at 40°C. The experimental weight loss in Part I of the TG curve is 3.25% and it is reasonable to assume oxalate dehydration. However, the entire Part I cannot be considered as dehydration, not only because the obtaining of anhydrous oxalate is impossible, but also because the DTA curve reveals an exothermic process of decomposition beyond 185°C. For this reason, we assume that the dehydration is in the range of 40 to 185°C, where the experimental weight loss is 2.5%, i.e., it strictly corresponds to the obtaining of $CuC_2O_4 \cdot 0.3H_2O$, most often reported as anhydrous oxalate [13–16].

Decomposition starts at 185°C (end of Part I), and it takes place up to 300°C. Judging from the TG curve, the process is quite slow in the beginning. The sample obtained isothermally at 200°C for 1 h shows an X-ray pattern (Fig. 1b) identical to that of the starting material, suggesting that a detectable decomposition has not occurred and confirming the fact reported in [19] that the X-ray pattern is unaffected by the water content. The slower decomposition process in air, as compared to the decomposition in N_2 and O_2 atmosphere, is established in a study of the process kinetics [26]. This is explained by the formation of copper nuclei, which grow thereafter. In air, these nuclei are poisoned by the instantaneous oxidation. This results in an increase of the activation energy of the process in air and its respective delay.

The abrupt decrease in weight (Part II) takes place in the range of 280–300°C and the experimental mass loss is 57.75%. If one assumes that only Cu is formed upon decomposition of $CuC_2O_4 \cdot 0.5H_2O$, the loss should amount to 60.4%. Taking into account that copper is partially oxidized during its formation, we assume that the product is Cu + $Cu_2O^{(1)}$ (calc. mass loss 57.12%).

In Part III (300–345°C), oxidation of the "non-oxidized" Cu to a secondary $Cu_2O^{(2)}$, and of the primary $Cu_2O^{(1)}$ to $CuO^{(1)}$ takes place (calc. mass gain 11.57%, exp. 11.71%). This is the part of the curve where the intensive (but incomplete) oxidation of Cu_2O to CuO has been observed using a copper foil [26]. Parts II and III are well distinct on the TG curve, but they result in one DTA peak at 330°C.

In Part IV (345–400°C), the experimental mass gain is 4.56%. Here, oxidation of $Cu_2O^{(2)}$ to $CuO^{(2)}$ (calc. mass gain 3.54%) takes place. In the experiment carried out in [26], this is the second part of the oxidation of CuO and at $T > 400$°C it is the only one.

The overall decomposition process, leading to CuO as the final product at $T = 400$°C, shows an experimental loss of 50.2%, the calculated value being 50.4%.

On the basis of the measurements of the magnetic susceptibility χ in the temperature range from –100 to 300°C, and the TG-analysis carried out during the magnetic measurement, the effective magnetic moment μ_{eff} is determined. In an octahedral crystal field, the theoretical effective magnetic moment μ_{eff}° for Cu(II) is temperature independent and depends only on the field strength. In a medium to strong octahedral crystal field, at a field strength of the order of 8000 cm^{-1}, the μ_{eff}° for Cu(II) is 2.08 BM. This means that if the Cu(II) is in the octahedral field, the experimental μ_{eff} should keep its value and the dependence $\chi = f(T)$ should obey the Curie-Weiss law. During the magnetic measurements of the samples, it was established that the Curie-Weiss law is violated and it follows that μ_{eff} is temperature dependent in the entire range studied (–100 to 300°C). Such a dependence has also been observed in [12, 14, 15] in the range from –200 to 50°C. It follows that the coordination of the Cu(II) ions is close to the tetrahedral or the square planar one, since under these coordination the effective magnetic moment depends on the temperature. The Cu(II) coordination is achieved due to the tetragonal deformation of the octahedral field as a result of the Jahn-Teller effect.

Fig. 5 compares the theoretical μ_{eff}° value for $CuC_2O_4 \cdot 0.5H_2O$, calculated at tetrahedral coordination of Cu(II) ions with the experimental μ_{eff}, determined at an unchanging value of the Weiss constant θ. In the determination of the experimental μ_{eff}, the change in the sample mass during the in situ measurements is taken into account and it is presented in the same figure. Furthermore, the magnetic measurements could be related

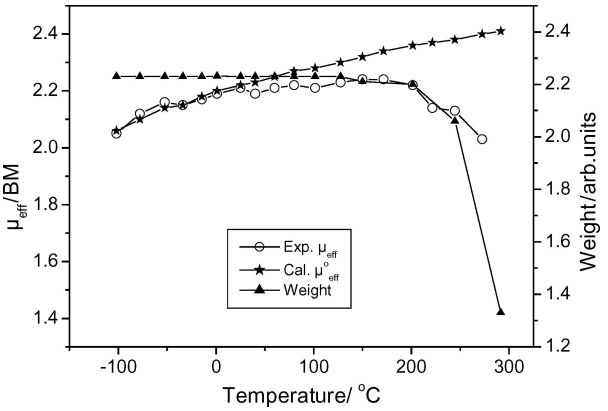

Figure 5 Temperature dependences of the calculated magnetic moment μ°_{eff}, the experimental magnetic moment μ_{eff} and the weight loss during in situ magnetic measurements of $CuC_2O_4 \cdot 0.5H_2O$.

in this way to the thermal analysis. Small differences in the TG-curves should be expected due to the different sample amounts and experimental procedure. The good correlation between the curves of μ°_{eff} and μ_{eff} (Fig. 5) confirms the conclusion concerning the tetrahedral-like symmetry of the field. The differences are observed upon the partial dehydration in the region 40–100°C most probably due to changes in the coordination of the copper(II) ions, suggesting that although the dehydration does not affect the X-ray patterns (Fig. 1b), *a*s well as the weight (Fig. 5), it obviously influences considerably the magnetic properties. After the small plateau, the experimental magnetic moment μ_{eff} increases quite slightly with temperature (at almost constant weight) and it should be noted that its trend is parallel to that of the theoretically calculated values.

About 200°C, similar to DTA, slow decomposition starts. Simultaneously, the decrease of μ_{eff} takes place. One of the reasons for this decrease could be the appearance of molecular antiferromagnetism between Cu(II)–Cu(II) ions, as also observed in the starting oxalate. However, taking into account the results of the thermal analysis, the more probable reason can be the appearance of the lower oxidation states Cu and Cu(I). It is known that they are diamagnetic and their effective magnetic moment equals zero, which explains the downward slope of the curve. The next similar experimental values of μ_{eff} can be explained by the already discussed oxidation of the copper nuclei formed, a process leading to an increase of the activation energy of the decomposition process and its respective delay. After the start of the rapid decomposition in the magnetic balance (over 240°C), the magnetic moment decreases.

On the basis of the DTA, TG and magnetic measurements, it can be concluded that the oxalate decomposition in air in Parts I and II obeys the following scheme (1), after which additional oxidation takes place.

$$3CuC_2O_4 \cdot 0.5H_20 \longrightarrow 3[Cu] \longrightarrow Cu + Cu_2O^{(1)} + 6CO_2 + 1.5H_2O \quad (1)$$

The separate parts (I–IV) of the TG curve can be related to the formation of the following solid products:

$$3\ CuC_2O_4.0.5H_20 \longrightarrow$$

$$\underset{\text{I + II}}{Cu + Cu_2O^{(1)}} \longrightarrow \underset{\text{III}}{0.5\ Cu_2O^{(2)} + 2\ CuO^{(1)}} \longrightarrow \underset{\text{IV}}{CuO^{(2)} + 2\ CuO^{(1)}} \quad (2)$$

The copper(II) oxide is finally obtained and the total weight loss after the last stage is 50.2%, the calculated value being 50.4%

3.2. Oxide product

On the basis of the conclusions concerning the oxalate decomposition for the synthesis of an oxide product for catalytic purposes, the temperature of 300°C and the duration of 1 h were chosen. This duration aims to avoid the product sintering, while at the chosen temperature it can be expected that Cu(I) will also be present in the sample. In some cases, the presence of Cu(I) enhances the catalytic activity [11, 38, 39]. In fact, the X-ray pattern (Fig. 1c) shows a great amount of monoclinic CuO (JCPDS No 48-1548) and less cubic Cu_2O (JCPDS No 78-2076). The results suggest that the temperature of 300°C and duration of 1 h are conditions sufficient for the decomposition of the oxalate, since the X-ray pattern does not reveal oxalate traces. This is a favorable result, taking into account that the degree of decomposition strongly depends on temperature [26]. The results show also that traces of elementary copper are not observed in the oxide product. However, the temperature of 300°C is insufficient for the complete oxidation of Cu_2O to CuO, which is achieved at 400°.

The oxide product obtained is studied by electron microscopy. Fig. 2b shows that the morphology of the initial oxalate is preserved, as well as the cavitational structure of the ellipsoids. On the other hand, the comparison of the particle size with that of the initial samples shows a decrease in size. The maximum in the size distribution is in the range 1–1.2 μm. The measured surface is 11 m^2/g and the pore volume is 0.08 cm^3/g. These values support the conclusion made on the basis of electron microscopy, since the largest portion of the pore volume is due to the volume between the particles.

The change in the magnetic susceptibility of the obtained highly disperse oxide product with temperature is depicted in Fig. 3, curve 2. CuO, as copper oxalate, also reveals a molecular antiferromagnetism [8]. For this reason, the trend of the curve $\chi = f(T)$ of the oxide product shows a broad plateau and a slightly expressed maximum, and is typical of a molecular antiferromegnet. Similar to the oxalate, here also the transition temperature strongly depends on the crystal size. The presence of a lesser amount of the diamagnetic Cu_2O in the sample leads to a decrease in the magnetic

susceptibility, as compared to that of pure CuO, and is the reason for the slightly expressed maximum.

4. Conclusions

1. The method chosen for the synthesis of copper oxalate leads to the obtaining of a precursor with a highly developed surface area and a satisfactory pore volume.

2. It is established, on the basis of magnetic measurements, that in the oxalate precursor the Cu(II) ions are in a tetrahedral-like coordination, resulting both from the strong tetragonal deformation of the octahedral field due to the Jahn-Teller distortion and from the stronger tendency of the oxalate ion to rotate around the C–C bond axis.

3. The results obtained suggest the impossibility to obtain a completely dehydrated oxalate and confirm that the X-ray pattern does not depend on the water content. However, a change in the magnetic properties is established during dehydration owing to changes in the coordination of the Cu(II) ions and in their interactions with surrounding ions.

4. The DTA and TG curves obtained and their comparison with the values of the calculated magnetic moment suggest that the final CuO is a secondary product of the decomposition of the copper oxalate, most probably taking place according to Scheme (1).

5. The results from the calculation of μ_{eff} during the decomposition process show that, in addition to the high specific surface, the proportion Cu(II)–Cu(I) can also be varied in the final product by varying the temperature range. This is interesting from the viewpoint of the application of the oxide product for catalytic purposes.

Acknowledgements

The authors wish to thank Dr. Anton Apostolov for the X-ray experiments and Silva Stanchovska for the magnetic measurements.

References

1. L. MARTA, O. HOROWITZ and M. ZAHARESCU, *Key Eng. Mat.* **132–136** (1997) 1239.
2. G. E. SHTER and G. S. GRADER, *J. Am. Ceram. Soc.* **77** (1994) 1436.
3. K. BERNARD and G. GRITZNER, *Phys. C., Supercond.* **196**(3/4) (1992) 259.
4. CONGKANG XU, YINGKAI LIU, GOUDING XU and GUANGHOU WANG, *Mat. Res. Bull.* **37** (2002) 2365.
5. M. POPA, J. M. CALDERON-MORENO, D. CRISAN and M. ZAHARESCU, *J. Therm. Anal. Calorimetry* **62** (2000) 633.
6. T. SPASOVA, M. KHRISTOVA, D. PANAYOTOV and D. MEHANDJIEV, *J. Cat.* **189** (1999) 43.
7. E. BEKYAROVA and D.MEHANDJIEV, in Proceedings of the 8th International Symposium on Heterogeneous Catalys (Varna, 1996) p. 787.
8. G. BLIZNAKOV, D. MEHANDJIEV and B. DYAKOVA, *Kinet. Katal.* **9** (1968) 269.
9. D. MEHANDJIEV and E. NICKOLOVA-ZHECHEVA, *Thermoch. Acta* **51** (1981) 343.
10. E. ZHECHEVA, S. ANGELOV and D. MEHANDJIEV, *ibid.* **67** (1983) 91.
11. A. M. DONIA, N. R. E. RADWAN and A. A. ATIA, *J. Therm. Anal. Calorimetry* **61** (2000) 249.
12. V. V. ZELENTZOV and T. G. AMINOV, *Dokl. Akad. Nauk SSSR* **158** (1964) 1393.
13. O. ASAI, M. KISHITA and M. KUBO, *J. Phys. Chem.* **63** (1959) 96.
14. L. DUBICKI, *Inorg. Chem.* **5** (1966) 93.
15. B. N. FIGGIS and D. J. MARTIN, *ibid.* **5** (1966) 100.
16. J. J. GIRERD, O. KAHN and M. VERDAGUER, *ibid.* **19** (1980) 274.
17. A. MICHALOWICZ, J. J. GIRERD and J. GOULON, *ibid.* **18** (1979) 3004.
18. A. GLEIZES F. MAURY and J. GALY, *ibid.* **19** (1980) 2074.
19. H. FICHTNER- SCHMITTLER, *Crystal Res. Technol.* **19** (1984) 1225.
20. H. SCHMITTLER, *Monatsber. Deut. Acad. Wiss. Berlin* **10** (1968) 581.
21. LE VAN MY, G. PERINET and P. BLANCO, *Bull. Soc. Chim. France* **361** (1969) 361.
22. K. P. PRIBYLOV and D. SH. FAZLULINA, *Zh. Inorg. Khim.* **14** (1969) 660.
23. K. NAGASE, K. SATO and N. TANAKA, *Bull. Chem. Soc. Japan* **48** (2) (1975) 439.
24. Y. A. UGAI, *Zh. Obshch. Khim.* **24** (1954) 1315.
25. R. PRASAD, *Thermoch. Acta* **406** (2003) 99.
26. D. BROADBENT, J. DOLLIMOR, D. DOLLIMOR and T. A. EVANS, *J. Chem. Soc. Faraday Trans.* **87**(1) (1991) 161.
27. P. PESHEV, G. GYUROV, Y. KHRISTOVA, K. PETROV, D. KOVACHVO, Y. DIMITRIEV, N. NENCHEVA and E. EVLAKHOR, *Mater. Res. Bull.* **23** (1988) 1765.
28. D. DOLLIMORE, *Thermoch. Acta* **177** (1991) 59.
29. *Idem.*, *ibid.* **117** (1987) 331.
30. V. V. BOLDYREV, I. S. NEVANCHEV, JU. I. MIHAYLOV and E. F. HAYRETDINOV, *Kinet. Katal.* **11** (1970) 367.
31. M. E. BROWN, D. DOLLIMORE and A. K. GALWEY, in "Comprehensive Kinetics, Reactions in the Solid State," edited by C.H. Bamford and C. F. H. Tipper (Elsevier, Amsterdam 1980) Vol. 22, p. 218.
32. H. J. T. ELLINGHAM, *J. Soc. Chem. Ind., (London)* **63** (1944) 125.
33. N. J. CARR and A. K. GALWEY, *J. Chem. Soc. Faraday Trans 1* **84**(5) (1988) 1357.
34. F. E. MABBS and D. J. MACHIN, in "Magnetism and Transition Metal Complexes" (Chapman & Hall, London, 1973) p. 153.
35. D. MEHANDJIEV and S. ANGELOV, in "Magnetochemistry of Solid State" (Nauka I Izkustvo, Sofia, 1979) p.116.
36. R. BOCA, in "Theoretical Foundations of Molecular Magnetism" (Elsevier, Amsterdam, Lousanne, New Yok, Oxford, Shannon, Singapore, Tokyo, 1999) p. 504.
37. UPAC (Fiz.Chem.Division), Recomandation 1984, *Pure Appl. Chem.* **57** (1985) 603.
38. T. TSONCHEVA, S. VANKOVA and D. MEHANDJIEV, *Fuel'82* (2003) 755.
39. V. RAKIC, V. DONDUR, S. GAJINOV and A. AUROUX, *Thermoch. Acta* **420** (2004) 51.

Received 1 November 2004
and accepted 14 February 2005